

# Evidence of an Internally Generated Optical-Dipole Potential in Matter-Wave Superradiance

Xinyu Luo,<sup>1</sup> L. Deng,<sup>2,3</sup> E.W. Hagley,<sup>2</sup> Kuiyi Gao,<sup>1</sup> Xiaorui Wang,<sup>1</sup> and Ruquan Wang<sup>1</sup>

<sup>1</sup>*Institute of Physics, Chinese Academy of Sciences, Beijing 100190, China*

<sup>2</sup>*Physical Measurement Laboratory, National Institute of Standards & Technology, Gaithersburg, Maryland USA 20899*

<sup>3</sup>*Center for Cold Atom Physics, Wuhan Institute of Physics and Mathematics, Chinese Academy of Science, Wuhan 430071, China*

(Dated: December 2, 2024)

We present the first experimental evidence supporting the postulation that an optical-dipole potential in a condensate undergoing superradiant scattering modifies the structure factor of the system and significantly impacts the scattering. Several consequences of this new detuning-dependent mechanism are discussed and verified experimentally. Our experiments indicate that whenever the generation and propagation growth of a new field are significant, the dynamic response of the condensate can have a profound impact on the scattering process.

PACS numbers: 03.75.-b, 42.65.-k, 42.50.Gy

Matter-wave superradiance is a unique light scattering process in which a long laser pulse interacting with an ultra cold atomic vapor results in discrete, collective, atom recoil motion. Since the first pioneering demonstration of this effect in a Bose condensate using red-detuned light in 1999 [1], there have been numerous theoretical studies of this intriguing process [1–9]. The widely-accepted theoretical framework developed over the last decade is based on the buildup of a self-reinforcing matter-wave grating that leads to high optical and matter-wave gain [1]. Except for a few numerical investigations [9], all studies [1–8] use rate equation treatments of atomic response that neglect the wave-propagation dynamics of the generated field. Correspondingly, these works, including the numerical simulations, predict that the scattering efficiency should not depend on whether the pump laser is detuned above or below the one-photon atomic resonance.

Recently, however, it was discovered that matter-wave superradiance was strongly suppressed over a wide detuning range when the pump light is tuned above the one-photon transition [10]. To explain this unexpected detuning asymmetry that challenged the pre-existing theoretical model, a new mechanism based on the ultra-slow propagation of an internally generated field was proposed [10, 11]. The central idea of this new mechanism is that this ultra-slowly propagating light field generates an important symmetry-breaking optical-dipole potential that dynamically modifies the condensate’s structure factor [12–14] and impacts the scattering rate at early times.

In this Letter we elaborate on the mechanism responsible for the symmetry breaking, and report the first supporting experimental evidence [10]. We begin by describing an intuitive physical picture of the process and discuss the vital role of the condensate’s chemical potential  $\mu$ . We show that the dynamic modification of  $\mu$  by the temporally and spatially dependent optical-dipole potential  $U_{\text{dipole}}(\mathbf{r}, t) \propto I_G(\mathbf{r}, t)/\delta$  alters the scattering dynamics and breaks the detuning symmetry (here,  $I_G(\mathbf{r}, t)$  is the generated-field intensity and  $\delta$  is the one-photon laser detuning). We demonstrate experimentally that as  $|\delta|$  in-

creases, the effect of  $U_{\text{dipole}}(\mathbf{r}, t)$  diminishes, resulting in an increase of superradiant scattering for blue-detuned pump light. Eventually, for very large  $|\delta|$  the effect of  $U_{\text{dipole}}(\mathbf{r}, t)$  becomes negligible and the scattering efficiency does not depend on the sign of the detuning. We also show that for a fixed single-photon Rayleigh scattering rate  $R_0$ , the restoration of detuning symmetry depends strongly on the condensate’s original chemical potential. The theoretical description and experimental evidence reported here provide insight into the underlying physics of this intriguing light-matter interaction process. Indeed, the newly proposed mechanism can profoundly alter the light scattering properties of a condensate, and may impact applications for superradiance in matter-wave interferometers and matter-wave amplifiers.

An intuitive view of the physical process can be obtained by first considering the generation and propagation of a new light field in a condensate during the light-scattering process [11]. First, a pump laser transfers momenta to atoms in a condensate via spontaneous Rayleigh scattering. However, unlike in a thermal gas, the scattering energy has an extra factor of the condensate’s average mean-field energy  $\bar{U}_{\text{mf}}$  due to the interatomic potential [15]. Furthermore, the extremely narrow two-photon resonance between the two motional states significantly modifies the atomic dispersion properties of the condensate [11]. This results in a drastic reduction of the propagation velocity of the scattered light as well as coherent propagation gain for the generated field. Under these conditions the new field grows diabatically (with respect to atomic motion), and generates a significant  $U_{\text{dipole}}(\mathbf{r}, t)$  that breaks the detuning symmetry. With red detunings the growing *attractive*  $U_{\text{dipole}}(\mathbf{r}, t)$  tends to cancel the additional energy due to the exchange interaction whereas with blue detunings the *repulsive*  $U_{\text{dipole}}(\mathbf{r}, t)$  augments this additional energy.

This intuitive picture can be further strengthened by examining the role of the condensate’s chemical potential  $\mu$  and structure factor  $S(\mathbf{k}, \mu)$  [12, 13] (see Fig. 1 and Ref. [16]). It has already been shown that  $S(\mathbf{k}, \mu) = S(\mu/E_r)$

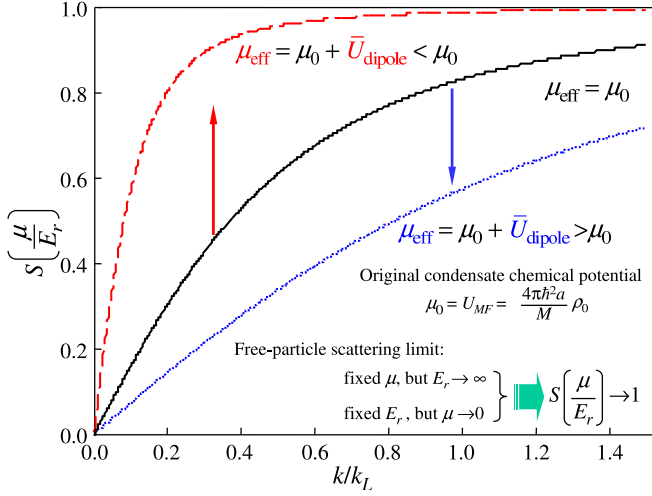


FIG. 1: Plot of the condensate's dynamic structure factor as a function of momentum transfer for different effective chemical potentials  $\mu_{\text{eff}}$  (in our experiments,  $k/k_L = \sqrt{2}$ ) [12, 13, 16]. A red-detuned  $U_{\text{dipole}}(\mathbf{r}, t)$  reduces  $\mu_{\text{eff}}$  as it grows, and the system approaches the “free-particle-scattering” limit earlier (top curve, red-dotted line). A blue-detuned  $U_{\text{dipole}}(\mathbf{r}, t)$  increases  $\mu_{\text{eff}}$ , leading to further suppression of scattering (bottom curve, blue-dot-dashed line). Note that even the initial spontaneous Rayleigh scattering process is impacted by  $S(\mathbf{k}, \mu_0)$  which always lowers the scattering rate (middle curve with no generated field where  $\mu_{\text{eff}} = \mu_0 = U_{\text{mf}} \approx (800 \text{ Hz})h$  for the condensates in this experiment).

(i.e., it is a function of  $\mu/E_r$  only, where  $E_r$  is the recoil energy of a scattered atom) modifies the rate of light scattering from a condensate [12–14, 17]. Usually, for fixed  $E_r$  the structure factor is assumed to be static. However, the growing time and spatially dependent  $U_{\text{dipole}}(\mathbf{r}, t)$ , which must now be included in the system Hamiltonian, will cause  $S(\mathbf{k}, \mu)$  to evolve. Because  $U_{\text{dipole}}(\mathbf{r}, t)$  is an internal potential, as it grows it will dynamically modify the original chemical potential  $\mu_0$  of the host condensate. This results in an effective, time-dependent chemical potential ( $\bar{U}_{\text{dipole}}(t)$  is the average optical-dipole potential)

$$\mu_{\text{eff}}(t) = \bar{U}_{\text{mf}} + \bar{U}_{\text{dipole}}(t), \quad (1)$$

and therefore an effective, time-dependent structure factor  $S(\mathbf{k}, \mu_{\text{eff}})$ . Correspondingly, the effective Rayleigh scattering rate becomes  $R_{\text{eff}} \rightarrow S(\mathbf{k}, \mu_{\text{eff}})R_0$ , where  $R_0 = |\Omega_L|^2 \Gamma / |2\delta|^2$ ,  $\Omega_L$  is the pump-laser Rabi frequency, and  $\Gamma \approx 2\pi \times 6 \text{ MHz}$  is the spontaneous decay rate of the upper electronic state.

It is well-known that  $S(\mathbf{k}, \mu)$  severely impacts low-momentum scattering (Fig. 1), and that for large momentum scattering  $S(\mathbf{k}, \mu) \rightarrow 1$  (i.e., as  $E_r \rightarrow \infty$  with  $\mu$  fixed), resulting in what is called the free-particle-scattering limit [12–14]. However, because  $S(\mathbf{k}, \mu)$  only depends on the ratio of  $\mu_{\text{eff}}/E_r$ , for fixed  $E_r$  the free-particle-scattering limit is also reached as  $\mu_{\text{eff}} \rightarrow 0$ . It is this limit that drives the scattering dynamics at early

times. From Ref. [11] the gain coefficient for the generated field becomes

$$G_{\text{eff}} \approx \frac{\kappa_0 \rho_0}{4\gamma\Gamma} S(\mathbf{k}, \mu_{\text{eff}}) R_0, \quad (2)$$

where  $\kappa_0 = 2\pi\omega_B |D|^2 / (c\hbar)$ ,  $\omega_B$  is the angular frequency of the generated field,  $D$  is the dipole-transition matrix element between the ground and excited electronic states,  $\rho_0$  is the original condensate density, and  $\gamma$  is the resonance linewidth of the two-photon momentum state.

It follows directly from Eq. (2) that any change in  $S(\mathbf{k}, \mu_0)$  will alter the exponential growth of  $U_{\text{dipole}}(\mathbf{r}, t)$  and impact the scattering process (Fig. 1). With a red-detuned pump, growth of the attractive  $U_{\text{dipole}}(\mathbf{r}, t)$  reduces  $\mu_0$  and brings  $S(\mathbf{k}, \mu_{\text{eff}})$  closer to unity for low-momentum transfers (Fig. 1, top curve), and hence increases the scattering efficiency. Once the generated field grows to a sufficient level in the high gain direction and enough atoms are scattered, the polarization term in Maxwell's equation starts to dominate [11] and this results in rapid growth of the optical and matter-wave fields. With a blue-detuned pump laser, however, the growing repulsive  $U_{\text{dipole}}(\mathbf{r}, t)$  increases  $\mu_{\text{eff}}$ , and leads to a reduction in  $S(\mathbf{k}, \mu_{\text{eff}})$  that lowers the scattering efficiency (Fig. 1, bottom curve). This impact on scattering efficiency at early times is the root of the observed asymmetry.

The existence of  $U_{\text{dipole}}(\mathbf{r}, t)$  and its effect on  $S(\mathbf{k}, \mu_0)$  has two direct implications. First, if  $R_0$  is held constant as  $\delta$  is varied, then  $U_{\text{dipole}}(\mathbf{r}, t)$  should be a monotonic function of  $\delta$ . Consequently, as  $|\delta|$  is increased, the effect of  $U_{\text{dipole}}(\mathbf{r}, t)$  should diminish and ultimately result in  $\mu_{\text{eff}} \rightarrow \mu_0 = \bar{U}_{\text{mf}}$ . We therefore expect the scattering efficiency for red detunings to drop slightly as  $|\delta|$  is increased because the negative impact of the original structure factor returns (Fig. 1, middle curve). Similarly, the scattering efficiency for blue detunings should grow to be the same as that of red detuning for the same reason. Second, if  $\mu_0$  is reduced by lowering the initial number of atoms  $N_0$  in the condensate while maintaining  $R_0$  fixed, the detuning at which red-blue symmetry is restored should correspondingly drop.

Experimentally, we first created an elongated condensate of  $^{87}\text{Rb}$  atoms using standard laser/radio-frequency cooling protocols [10]. A pump pulse of selected frequency, polarization, and duration was subsequently applied along the short axis of the condensate. The pump-laser intensity was actively stabilized to the  $\pm 2\%$  level because the experiments were carried out under the strict condition that  $R_0$  be held constant as the detuning was varied ( $|\Omega_L|^2 / |\delta|^2 = \text{const}$ ). The upper detuning used in these experiments was limited by our maximum pump power because of this constraint. Also,  $N_0$  was controlled to keep  $\mu_0$  constant. After application of the pump pulse, the magnetic trap was turned off and absorption imaging was employed subsequent to a delay sufficient to allow spatial separation of the scattered components.

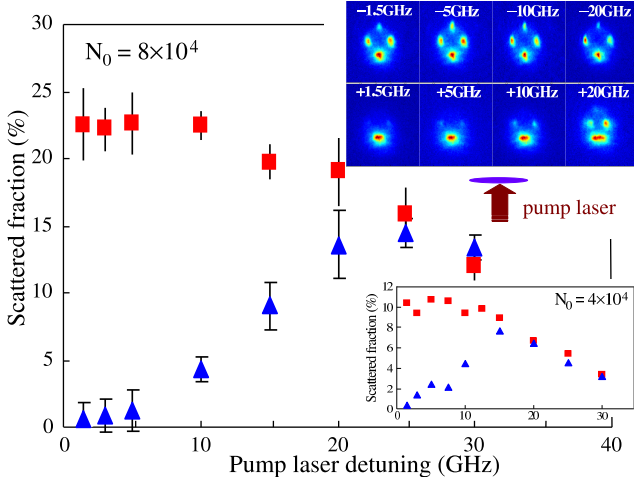


FIG. 2: Plot of matter-wave scattering with red and blue detunings over a wide pump-laser detuning range with a condensate of  $N_0 = 8 \times 10^4$  atoms.  $R_0 = 34$  Hz, the pump-pulse duration was  $\tau = 500 \mu\text{s}$ , and each data point is the average of five runs. Upper insert: TOF (15 ms) images showing the effect of  $U_{\text{dipole}}$  at various red and blue detunings. Note the differences between the red and blue images for the same  $|\delta|$ . The image field of view is  $560 \mu\text{m}$  by  $627 \mu\text{m}$ . Lower inset: Parameters same as those of the main plot except  $N_0 = 4 \times 10^4$ . Here the onset of detuning symmetry occurs at smaller detunings because  $\mu_0$  is smaller.

The main plot of Fig. 2 shows the atom scattering efficiency as a function of laser detuning with a condensate initially containing  $N_0 = 8 \times 10^4$  atoms.  $R_0 = 34$  Hz was maintained as the detuning was varied so that in the absence of any impact on scattering from  $S(\mathbf{k}, \mu)$ ,  $U_{\text{dipole}}(\mathbf{r}, t)$  would simply be a monotonic function of laser detuning. As  $|\delta|$  was increased on the red side of the transition, the effect of  $U_{\text{dipole}}(\mathbf{r}, t)$  diminished and  $S(\mathbf{k}, \mu_{\text{eff}})$  returned to its initial value (Fig. 1), causing the scattering efficiency to drop slightly. With a blue-detuned pump, however, we observed a marked increase in superradiant scattering as the detuning increased. At large blue detunings the atom scattering efficiency was comparable to the red-detuned case, indicating that the impact of  $U_{\text{dipole}}(\mathbf{r}, t)$  was small and that  $\mu_{\text{eff}}$  and  $S(\mathbf{k}, \mu_{\text{eff}})$  were basically unchanged from their original values, as predicted by Ref. [10]. The lower insert of Fig. 2 shows that symmetry is restored at a much smaller  $|\delta|$  when  $N_0$  is reduced by a factor of two. This effect is also in accord with our original postulation [10]. There is, however, an unexplained roll-off in scattering efficiency at very large detunings for both sets of data. In addition, the size of the condensate after scattering and the position of the scattered components are different for red and blue detuning (see 20 GHz data in upper insert of Fig. 2). We suspect that these effects are due to the pump laser because the intensity had to be increased by a factor of 400 to maintain  $R_0 = 34$  Hz as  $|\delta|$  was increased from 1.5 GHz to 30 GHz. Correspondingly, any optical-dipole force due to a mild focusing or

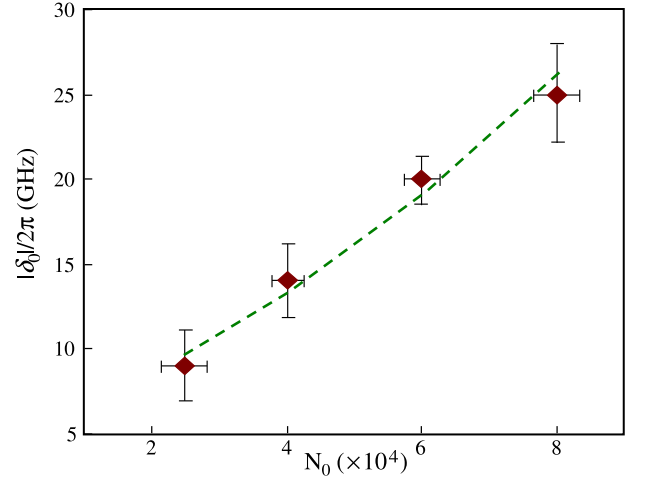


FIG. 3: Plot of pump-laser onset detuning  $|\delta_0|/2\pi$  (filled diamonds) beyond which symmetry is restored as a function of  $N_0$  with  $R_0 = 34$  Hz. The dotted line is a fit using a Thomas-Fermi calculation with wave-propagation effects included.

the turn-on characteristics of the pump would increase by a factor of twenty as the detuning was scanned under our experimental conditions.

Figure 3 is a plot of the pump-laser onset detuning  $|\delta_0|/2\pi$  at which symmetry is restored as a function of atom number while holding  $R_0 = 34$  Hz constant. From Eq. (1) the onset pump-laser detuning for symmetry restoration can be expressed as  $|\delta_0| = \text{const.} \times I_G(\rho_0, S(\mu_{\text{eff}}/E_r))/|\mu_{\text{eff}} - \mu_0|$  under the condition that  $|\mu_{\text{eff}} - \mu_0|/\mu_0 < 1$ . In the Thomas-Fermi limit  $\rho_0 \propto N_0^{2/5}$ , and therefore  $|\delta_0| \propto \exp[c_0 N_0^{2/5} S(\mu_{\text{eff}}/E_r)]/N_0^{2/5}$  ( $N_0 \gg 1$ ,  $c_0$  is a constant) when wave-propagation effects are included. The data in Fig. 3 are in good agreement with a fit using this model, but not when wave-propagation effects are neglected. This is strong evidence in support of Eq. (1) and our theory about the underlying physical mechanism in matter-wave superradiance with condensates.

Figure 4(a) is a plot of the scattering efficiency versus pump-pulse duration at a fixed detuning with  $R_0 = 39$  Hz. As the pump duration was increased the total scattering increased and then saturated for both red and blue detunings, as in the original study (red detunings only) [1]. We point out that potential four-matter-wave mixing [19], reabsorption of the generated field, as well as the overlap time of the scattered components all contribute to the observed saturation behavior. Figure 4(b) shows the scattering efficiency as a function of  $N_0$  under the conditions of fixed detuning  $\delta$ , scattering rate  $R_0$ , and pump duration  $\tau$ . The dashed curve exhibits growth characteristics typical of nonlinear optical wave-mixing processes when wave-propagation effects are important [20]. In fact, the linear portion of this curve would be steeper were it not for the impact of  $S(\mathbf{k}, \mu_{\text{eff}})$ . This again indicates that matter-wave superradiance results from a nonlinear wave-mixing and propagation process. Indeed,

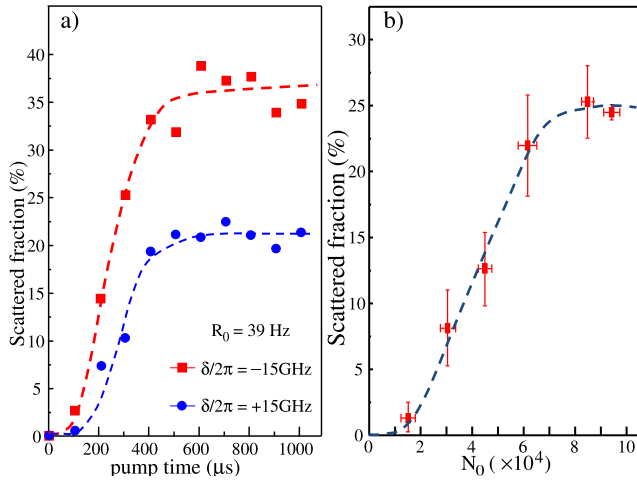


FIG. 4: a) Matter-wave scattering efficiency as a function of pump duration for red and blue detunings when  $N_0 = 8 \times 10^4$ . b) Matter-wave scattering efficiency as a function of  $N_0$  with  $R_0 = 34$  Hz,  $\tau = 500$   $\mu$ s, and  $\delta/2\pi = -15$  GHz. Dashed curves are guides.

when the well-known nonlinear wave-mixing and propagation theory is generalized to include atomic center-of-mass motion, it can satisfactorily explain the genesis of matter-wave superradiance in both bosonic and fermionic [21] systems. The detuning asymmetry observed in condensates is simply a consequence of the interplay between the wave propagation process and the internal structure (properties) of the condensate.

In conclusion, we presented the first experimental evidence that matter-wave superradiance results from an ultra-slowly propagating, internally generated field in a condensate. Our work reveals that the optical-dipole potential of this field dynamically modifies  $\mu$  and  $S(\mathbf{k}, \mu)$  of the original condensate and alters the scattering dynamics at early times. This implies that whenever the

propagation growth of a new field is significant, the dynamic response of the condensate itself must be taken into account. Correspondingly, a host of well-known gaseous-phase nonlinear optical phenomena [20] should be re-examined in the context of Bose condensates. We note that a detailed analytical treatment of matter-wave superradiance is very difficult. The spatial- and time-dependent nature of the optical-dipole potential resulting from rapid coherent growth of the generated field, and its dynamic effect on the condensate's structure factor, make an analytical solution improbable. However, many interesting questions still need to be addressed. For example, could a multi-component superfluid theoretical approach shed additional light on the scattering dynamics? How does the change in the effective chemical potential affect the structure factor in a lower-dimensional system? Furthermore, what would happen to the red-blue detuning asymmetry if the condensate had a negative scattering length? Finally, we point out that in condensed matter physics the structure factor of the medium is usually regarded as a static quantity. Our results have shown, however, that when the generation and propagation of a new light field are important, the condensate structure factor evolves dynamically. Therefore, if a condensate is used to study condensed matter physics, the consequences of the evolving structure factor must also be considered. We hope that this study will prompt future experimental and theoretical investigations of this intriguing topic.

**Acknowledgments:** We thank Dr. Charles Clark (NIST), Dr. Eite Tiesinga (NIST), Dr. Joshua Bienfang (NIST), and Prof. M.G. Payne for discussions. We also thank Mr. Xiong Huang for assistance with the experiments. Ruquan Wang acknowledges financial support from the National Basic Research Program of China (973 project Grant No. 2006CB921206), the National High-Tech Research Program of China (863 project Grant No. 2006AA06Z104), and the National Science Foundation of China (Grant No. 10704086).

- 
- [1] S. Inouye et al., *Science* **285**, 571 (1999).
  - [2] W. Ketterle and S. Inouye, *C.R. Acad. Sci. Paris t .2*, **IV**, 339 (2001).
  - [3] M.G. Moore and P. Meystre, *Phys. Rev. Lett.* **83**, 5202 (1999).
  - [4] Ö.E. Mstecaplioglu and L. You, *Phys. Rev. A* **62**, 063615 (2000).
  - [5] N. Piovella et al., *Opt. Commun.* **187**, 165 (2001).
  - [6] H. Pu, W. Zhang, and P. Meystre, *Phys. Rev. Lett.* **91**, 150407 (2003).
  - [7] R. Bonifacio et al., *Opt. Commun.* **233**, 155 (2004).
  - [8] C. Benedek and M. G. Benedikt, *J. Opt. B: Quantum Semiclass. Opt.* **6**, S111 (2004).
  - [9] O. Zobay and G. M. Nikolopoulos, *Phys. Rev. A* **73**, 013620 (2006); Yu.A. Avetisyan and E.D. Trifonov, *Laser Physics Letters* **1**, 373 (2004). These studies contain numerical calculations of Maxwell's wave equation.
  - [10] L. Deng et al., *Phys. Rev. Lett.* **105**, 220404 (2010).
  - [11] L. Deng, M.G. Payne, and E.W. Hagley, *Phys. Rev. Lett.* **104**, 050402 (2010).
  - [12] F. Zambelli et al., *Phys. Rev. A* **61**, 063608 (2000).
  - [13] J. Steinhauer et al., *Phys. Rev. Lett.* **88**, 120407 (2002).
  - [14] D.M. Stamper-Kurn et al., *Phys. Rev. Lett.* **83**, 2876 (1999).
  - [15] G.K. Campbell et al., *Phys. Rev. Lett.* **94**, 170403 (2005).
  - [16] We plot  $S(\mathbf{k}, \mu_{\text{eff}})$  from Ref. [12] to show the impact of  $\mu_{\text{eff}}$ . The form of  $S(\mathbf{k}, \mu_{\text{eff}})$  when the generated field has a fixed, high gain propagation direction may be different.
  - [17] Stamper-Kurn Ph.D. Thesis, see <http://cua.mit.edu>
  - [18] S. Wolf et al., *Phys. Rev. Lett.* **85**, 4249 (2000).
  - [19] L. Deng et al., *Nature (London)* **398**, 218 (1999).
  - [20] L. Deng, M.G. Payne, and W.R. Garrett, *Physics Reports*, **429**, 123 (2006).
  - [21] We also have experimental evidence of collective atom recoil motion with fermions (submitted, *Phys. Rev. Lett.*).